On the Performance of Cooperative Spectrum Sensing in Random Cognitive Radio Networks

On the Performance of Cooperative Spectrum Sensing in Random Cognitive Radio Networks

Yibo He[†], *Student Member, IEEE*, Jiang Xue[†‡], *Member, IEEE*, Tharmalingam Ratnarajah[†], *Senior Member, IEEE*, Mathini Sellathurai[§], *Senior Member, IEEE* and Faheem Khan[†], *Member, IEEE*

***Abstract*—This paper investigates the performance of cooperative spectrum sensing in cognitive radio networks using the stochastic geometry tools. In order to cope with the diversity of received signal-to-noise ratios (SNRs) at secondary users, a practical and efficient cooperative spectrum sensing model is proposed and investigated based on the generalized likelihood ratio test (GLRT) detector. In order to investigate the cooperative spectrum sensing system, the theoretical expressions of the probabilities of false alarm and detection of the local decision are derived. The optimal number of cooperating secondary users is then investigated to achieve the minimum total error rate of the final decision by assuming that the secondary users follow a homogeneous Poisson point process (PPP). Moreover, the theoretical expressions for the achievable ergodic capacity and throughput of the secondary network are derived. Furthermore, the technique of determining an appropriate number of cooperating secondary users is proposed in order to maximize the achievable ergodic capacity and throughput of the secondary network based on a target total error rate requirement. The analytical and simulation results validate the chosen optimal number of collaborating secondary users in terms of spectrum sensing, achievable ergodic capacity and throughput of the secondary network.**

***Index Terms*—Cognitive radio, spectrum sensing, ergodic capacity, throughput, Poisson point process.**

I. Introduction

In recent years, the explosive growth of wireless data traffic has led to spectrum scarcity due to ever-increasing demand for additional spectrum to provide new wireless services and applications. Cognitive radio (CR) has been put forward as a promising solution to end the spectrum scarcity, existing mainly due to rigid spectrum allocation policies. CR allows the secondary (unlicensed) users (SUs) to use the available spectrum opportunities when primary (licensed) users (PUs) are inactive, based on the condition that secondary transmission must not cause harmful interference to PUs. It is therefore of utmost importance to develop highly reliable and efficient spectrum sensing techniques which are crucial to the implementation of CR system and other CR-based derivatives, such as licensed shared access (LSA) [1].

A. Related Work

The objective of spectrum sensing is to determine whether the PU is present so that the SU can decide when to access the licensed frequency bands. Generally, spectrum sensing techniques utilize single node or cooperative spectrum sensing. Cooperative spectrum sensing technique can improve the performance of the spectrum sensing system [2] by making a final decision on the status of the PU in a centralized or distributed manner. Many different combining techniques, fusion strategies and sensing techniques have been proposed to improve the accuracy and efficiency of cooperative spectrum sensing [3]–[11]. The sensor selection method was investigated in [12] in order to obtain spatially independent sensors. In [13], the sensing throughput trade-off of the secondary network was studied based on energy detector (ED). The performance of cooperative spectrum sensing with ED was investigated in [14] based on the constant detection rate (CDR) and the constant false alarm rate (CFAR) requirements when the SUs were distributed randomly. Besides, the optimization of cooperative spectrum sensing with ED was studied in [15], but the locations of SUs were assumed to be identical and fixed.

Meanwhile, the stochastic geometry approach using Poisson point process (PPP) has been used to analyze the performance of random wireless networks and CR networks [16]–[19]. In [20], the spectrum-sharing transmission capacity was investigated by applying stochastic geometry in overlay and underlay CR networks and the optimal spatial density was derived in order to achieve the maximum sum spectrum-sharing transmission capacity. Khoshkholgh *et al.* [21] analyzed the outage performance and mean spatial throughput of the primary network in CR networks by utilizing stochastic geometry. Peng *et al.* [22] derived the ergodic capacity achieved by the single nearest and Nth-nearest remote radio head (RRH) association strategies in cloud radio access networks and investigated the impact of RRH density and number of antennas per RRH on the ergodic capacity gain. In [23], the interference in CR networks was investigated when the PPP of PUs and the Poisson hole process of the SUs were dependent and the interference was estimated well by utilizing Poisson cluster process to model the Poisson hole process.

Besides, in the existing works, multi-channel CR network has been exploited [24]–[27]. In [24], a semi-distributed cooperative spectrum sensing protocol was proposed and the throughput maximization issue was investigated from the perspectives of the channel assignment, the spectrum sensing time and the access parameters. The total transmit capacity over all the subchannels for the secondary network was studied in [25] under the transmit power and the interference power constraints. In order to improve the sensing reliability, a spatial-spectral joint detection approach was proposed in [26]

Manuscript received...This work is supported by the Seventh Framework Programme for Research of the European Commission under grant number ADEL-619647.

[†]Y. He, J. Xue, T. Ratnarajah and F. Khan are with the Institute for Digital Communications (IDCOM), School of Engineering, The University of Edinburgh, Edinburgh, UK.

[§]Mathani Sellathurai is with the School of Engineering and Physical Sciences, Heriot-Watt University, Edinburgh, UK, e-mail: m.sellathurai@hw.ac.uk.

‡ is the correspondence author.

for multi-channel spectrum sensing. But we focus on the narrowband spectrum sensing in this paper, since the single-channel spectrum sensing performance with the homogeneous PPP still needs certain further exploration and the results in this paper are also valid for wideband spectrum sensing when the subchannel is sensed in a sequential manner.

B. Motivations

This paper investigates the cooperative spectrum sensing with the generalized likelihood ratio test (GLRT) eigenvalue based detector in interweave CR networks while assuming that the SUs follow a homogeneous PPP and this is motivated by multiple factors. Firstly, it is more practical to assume SUs follow a homogeneous PPP compared with the traditional assumption in the literatures. Most of the previous works assumed that the received SNRs at SUs were identical, but in practice the received SNRs could vary depending on the locations of SUs. Secondly, cooperative spectrum sensing with PPP is a challenging topic and still needs further investigations. Specifically, a new strategy is required to cope with the diversity of the received SNRs in PPP model, which has not been studied in the literatures. Thirdly, the existing works are mainly based on ED when the stochastic geometry is employed, but one of the limitations of the ED based methods is the sensitivity to the noise uncertainty. Therefore, the robust GLRT detector [28] is employed to evaluate the cooperative spectrum sensing and secondary transmission performances. Lastly, a minimum total error rate considers the benefits of PUs and SUs simultaneously, but the previous works such as [29], [30] mainly focused on the probability of false alarm due to the lack of generalized closed-form expression of the detection probability, which only considered the interests of SUs. A low probability of false alarm can make SUs have more chances to access the spectrum holes, however, the benefits of PUs may not be guaranteed. Therefore, the aforementioned issues motivate us to investigate the total error rate performance and the optimality of cooperative spectrum sensing system with the GLRT detector by applying stochastic geometry, which considers the benefits of PU and SUs concurrently.

C. Main contributions

The main contributions of this paper can be summarized as follows.

- Firstly, the sensing performance of each SU based on the GLRT detector is investigated as cooperative spectrum sensing requires sensing by each node. We derive the generalized closed-form expressions of probabilities of false alarm and detection of the GLRT detector for each SU, which is required to analyze the total error rate, achievable ergodic capacity and throughput. Unlike the theoretical expressions on the sensing performance provided in [30], [31], the expressions derived in this paper are with low computational complexity and valid for the general case with an arbitrary number of receive antennas.
- Secondly, an efficient GLRT-based cooperative spectrum sensing technique is proposed by using stochastic geometry, which can utilize only a few, not always all, SUs to achieve the minimum total error rate. Meanwhile, the optimal number of the cooperating SUs is also studied, which enables the total error rate to achieve the minimum value. Therefore, the speed and accuracy of cooperative spectrum sensing is improved compared to the cooperation among all SUs, when sending local decisions in different time slots is chosen for decision combining.
- Finally, in order to maximize the achievable ergodic capacity and throughput of the random secondary network, effective methods are proposed for different fusion rules to determine the appropriate number of cooperating SUs when the target total error rate is not exceeded.

D. Mathematical Notations

Throughout the paper, vectors are denoted by lower-case boldfaced characters and matrices are represented by upper-case boldfaced characters. The notation $|\cdot|$ denotes the magnitude operator. The $\boldsymbol{A}^{\dagger}$ denotes the conjugate transpose of matrix $\boldsymbol{A}$. $\hat{a}$ and $\overline{a}$ are the estimated parameter and average value, respectively. The notation $\otimes$ is the Kronecker product. The identity matrix of size N is $\boldsymbol{I}_N$, and $\mathbf{0}$ is the null vector (or matrix). The notation $\mathbb{E}[\cdot]$ is the statistical expectation operator. The complex normal distribution with mean $\boldsymbol{\mu}$ and covariance matrix $\boldsymbol{\Sigma}$ is $\mathcal{CN}(\boldsymbol{\mu}, \boldsymbol{\Sigma})$. The central Wishart distribution with parameters a, b and $\boldsymbol{\Sigma}$ is $\mathcal{CW}_a(b, \boldsymbol{\Sigma})$ where $\boldsymbol{\Sigma}$ is an $a \times a$ positive definite covariance matrix. Other special functions (please refer to [32] for more information on special functions) used throughout the paper include

- $(\cdot)_a$ is the Pochhammer symbol.
- $\Gamma(\cdot)$ is the gamma function.
- $\Phi(\cdot)$ is the error function and $\Phi(y) \triangleq \frac{2}{\sqrt{\pi}} \int_0^y e^{-t^2} \mathrm{d}t$.
- $I^{-1}(z, a, b)$ is used to denote inverse regularised incomplete Beta function $I_z^{-1}(a, b)$ for convenience.
- ${}_2F_1(\cdot, \cdot; \cdot; \cdot)$ is the Gaussian hypergeometric function.
- $G_{p,q}^{m,n}\left(\begin{matrix} a_1, \ldots, a_p \\ b_1, \ldots, b_q \end{matrix} \middle| \, z\right)$ is the Meijer G-function.

The remainder of this paper is organized as follows. Section II describes the system model of cooperative spectrum sensing based on the GLRT detector. Section III derives the closed form expressions of the probabilities of detection and false alarm when utilizing the GLRT detector and investigates the optimal number of collaborating SUs. The achievable ergodic capacity and throughput of the secondary network are analyzed in section IV. Section V presents the simulation results and discussions and section VI concludes this paper.

II. System Model

We consider a centralized cooperative spectrum sensing system with decision fusion, shown in Fig. 1. The fusion center (FC) is used to collect the decisions made by the SUs to make a final decision. The SUs which are used to sense the status of PU are comprised of certain RRHs or user equipments (UEs). During the cooperative spectrum sensing process, each SU within the coverage radius of the FC detects the status of the PU independently and then sends the detection result to the FC. After that, the FC gives a final decision on the status of the PU through an appropriate voting rule. The PU is assumed to be equipped with single antenna and each SU has multiple antennas.

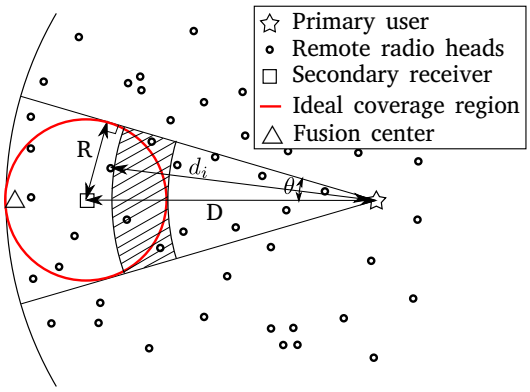

Fig. 1. The system model

A practical assumption is that the SUs are uniformly distributed on a 2-dimensional plane $\mathbb{R}^2$ based on a homogenous PPP with density ρ. According to Palm theory, the SUs located within the coverage radius of the FC follow the same PPP. The coverage radius of the FC is denoted by R and the distance between the PU and the secondary receiver located at the origin of the coverage area of the FC is represented by D. Since only the SUs within the coverage radius of the corresponding FC can be collaborated together to detect the status of the PU, we only consider the SUs that are located within the area of interest in this work. Assuming the transmitted signals between the PU and secondary network experience path loss and Rayleigh fading, the received signal power at the ith SU can be given as

$$P_i = \frac{P_{\mathrm{T}}}{d_i^{\varepsilon}}\omega_i, \tag{1}$$

where ω_i denotes the Rayleigh fading gain and follows the Gamma distribution when maximal ratio combining (MRC) is used to achieve full diversity gain, i.e., $\omega_i \sim \Gamma(m,1)$, m is the number of receive antennas of each SU, P_{T} denotes the PU's signal power, d_i means the distance between the PU and the ith nearest SU from the PU and ε is the path loss exponent factor. The shadowing area in Fig. 1 is defined as the region whose distance is equal or greater than $D-R$ but less than $d_i - D + R$. The PDF of ω_i can be written as

$$f_{\omega_i}(\omega) = \frac{\omega^{m-1}e^{-\omega}}{(m-1)!}. \tag{2}$$

The spectrum sensing between each SU and the PU is assumed to be a GLRT-based sensing system with m receive antennas. Let $\mathcal{H}_0$ (PU is absent) and $\mathcal{H}_1$ (PU is present) denote the null and the alternate hypotheses. During the sensing period, the matrix of received signal samples, $\mathbf{Y} \in \mathbb{C}^{m\times n}$, at the SU is

$$\mathcal{H}_0 : \mathbf{Y} = \mathbf{V}, \tag{3a}$$
$$\mathcal{H}_1 : \mathbf{Y} = \mathbf{h}\mathbf{s}^{\dagger}d^{-\frac{\varepsilon}{2}} + \mathbf{V}, \tag{3b}$$

where n is the sample number, $\mathbf{V} \in \mathbb{C}^{m\times n}$ represents the samples from a circularly symmetric complex additive white Gaussian noise (AWGN) process, where $\mathbf{V} \sim \mathcal{CN}\left(\mathbf{0}, \sigma_v^2\mathbf{I}_m \otimes \mathbf{I}_n\right)$, $\mathbf{s} \sim \mathcal{CN}\left(\mathbf{0}, P_{\mathrm{T}}\mathbf{I}_n\right) \in \mathbb{C}^{n\times 1}$ is the transmit signal of the PU. Finally, $\mathbf{h} \in \mathbb{C}^{m\times 1}$ is the channel vector. Henceforth, the covariance matrix of $\mathbf{Y}$, $\mathbf{R}_{yy} = \mathbb{E}[\mathbf{Y}\mathbf{Y}^{\dagger}]$, is given by

$$\mathcal{H}_0 : \quad \mathbf{R}_{yy} = \sigma_v^2\mathbf{I}_m, \tag{4a}$$
$$\mathcal{H}_1 : \quad \mathbf{R}_{yy} = P_{\mathrm{T}}d^{-\varepsilon}\mathbf{h}\mathbf{h}^{\dagger} + \sigma_v^2\mathbf{I}_m. \tag{4b}$$

Within the sensing duration of n samples, the sample covariance matrix estimated from $\mathbf{Y}$ is $\widehat{\mathbf{R}}_{yy} = \frac{1}{n}\mathbf{Y}\mathbf{Y}^{\dagger}$. Thus $\mathbf{W} = n\widehat{\mathbf{R}}_{yy} = \mathbf{Y}\mathbf{Y}^{\dagger} \in \mathbb{C}^{m\times m}$ is a complex Wishart matrix. Also, let $\hat{\lambda}_{\min} = \hat{\lambda}_m < \cdots < \hat{\lambda}_1 = \hat{\lambda}_{\max}$ be the eigenvalues, in increasing order, estimated from $\widehat{\mathbf{R}}_{yy}$. The decision statistic for the GLRT-based eigenvalue detector is given by $T_{\mathrm{GLRT}} = \frac{\hat{\lambda}_{\max}}{\sum_{l=1}^{m}\hat{\lambda}_l}$.

III. Sensing Performance Analysis Based On Stochastic Geometry

In this section, an efficient cooperative spectrum sensing technique is proposed while achieving the minimum total error rate of the final decision. Firstly, collaborating all the possible SUs to implement cooperative spectrum sensing can not always achieve the best performance due to the diversity of the SNRs received at SUs. An SU with very low received SNR can be classified as an unreliable node and may degrade the cooperative sensing performance. Secondly, combining all the local spectrum sensing decisions concurrently at the fusion center can lead to the high design complexity and the waste of bandwidth, such as sending local decisions on orthogonal frequency bands. Hence, sending different local decisions in different time slots is chosen in this work, but this may affect the sensing speed. However, according to the IEEE 802.22 standard for Wireless Regional Area Networks (WRANs) [33], the SUs have to vacate the licensed frequency bands as soon as possible once the PU is active. Therefore, in order to address the two issues mentioned above, an efficient cooperative spectrum sensing technique using different time slots to receive local decisions is proposed to guarantee the accuracy and speed of the sensing process. Furthermore, the statistical optimal number of the cooperating SUs k_{opt} is studied, which can make the total error rate achieve the minimum value when the number of available SUs is large.

A. Distributions On The GLRT Detector

Both the probabilities of detection and false alarm of an individual SU are required to investigate the total error rate and transmission performance of secondary network in CR networks. Therefore, we derive the probability of detection $P_{\mathrm{d},i}^{\mathrm{su}}$ and probability of false alarm $P_{\mathrm{fa},i}^{\mathrm{su}}$ seen at the ith SU in this subsection. The sensing error probabilities seen at the FC will be discussed in the next subsection when considering decision reporting errors.

Theorem 1: The closed-form expression of the probability of false alarm seen at the ith SU using the GLRT detector with m receive antennas, i.e., $P_{\mathrm{fa},i}^{\mathrm{su}}$, is given by

$$P_{\mathrm{fa},i}^{\mathrm{su}}(r_i) = 1 - \frac{\Gamma(mn)(m\eta)^{-\xi}}{\xi\Gamma(mn-\xi)\Gamma(\xi)}\left(\mathbf{\Delta}(r_i) - \mathbf{\Delta}\left(\frac{1}{m}\right)\right), \tag{5}$$

where $\frac{1}{m} \le r_i \le 1$ denotes the decision threshold of ith SU and $\mathbf{\Delta}(\cdot)$ is defined by

$$r_i = \eta I^{-1}\left(\frac{\Gamma(mn)(m\eta)^{-\xi}}{\xi\Gamma(mn-\xi)\Gamma(\xi)}\left(\mathbf{\Delta}\left(\frac{1}{m}\right)+(1-P_{\mathrm{fa},i}^{\mathrm{su}})\frac{\xi\Gamma(mn-\xi)\Gamma(\xi)}{\Gamma(mn)(m\eta)^{-\xi}}\right),\xi,mn-\xi\right). \tag{9}$$

$$r_i = \left(\frac{1}{2}\left(\sum_{t=0}^{\infty}\frac{C_t\sqrt{\varphi_i}}{2t+1}\left[\frac{\sqrt{\pi}}{2}\Phi\left(\tau_i\sqrt{\varphi_i}+\frac{1}{2(m-1)\varphi_i}\right)+\sqrt{\pi}(1-P_{\mathrm{d},i}^{\mathrm{su}})\right]^{2t+1}-\tau_i\varphi_i\right)^{-1}+1\right)^{-1}, \tag{13}$$

$$\mathbf{\Delta}(y) = {}_2F_1\left(\xi,1+\xi-mn;\xi+1;\frac{y}{\eta}\right)(my)^{\xi}, \tag{6}$$

where η and ξ are given by

$$\eta = \frac{0.8132b^2}{a-1.7711b}, \quad \xi = \frac{(a-1.7711b)^2}{0.8132b^2}, \tag{7}$$

and a, b are defined as

$$a = (\sqrt{m}+\sqrt{n})^2, \quad b = (\sqrt{m}+\sqrt{n})\left(\sqrt{\frac{1}{m}}+\sqrt{\frac{1}{n}}\right)^{\frac{1}{3}}. \tag{8}$$

Proof: The proof is shown in the Appendix A. ■

Hence, for a complex Gaussian signal, the decision threshold r_i with respect to the individual probability of false alarm seen at the ith SU can be calculated by (9) at the top of this page. This expression is used to calculate the required decision threshold for a desired false alarm rate, which is necessary for the individual and cooperative spectrum sensing under the CFAR requirement. The proof of Eq. (9) is provided in the Appendix B.

Theorem 2: The detection probability $P_{\mathrm{d},i}^{\mathrm{su}}$ seen at the ith SU using the GLRT detector is derived as

$$P_{\mathrm{d},i}^{\mathrm{su}}(r_i) = 1-\frac{1}{2}\left[\Phi\left(\tau_i\sqrt{\varphi_i}+\frac{r_i}{2\sqrt{\varphi_i}(1-r_i)}\right)-\Phi\left(\tau_i\sqrt{\varphi_i}+\frac{1}{2(m-1)\sqrt{\varphi_i}}\right)\right], \tag{10}$$

where τ_i and φ_i are given by

$$\tau_i = n(m-1)\left(\frac{1}{mn\gamma_i}-\frac{1}{1+m\gamma_i}\right)\left(1+\frac{m-1}{mn\gamma_i}\right), \tag{11}$$

$$\varphi_i = \frac{1}{2n(m-1)^2}\left(\frac{1}{1+m\gamma_i}-\frac{1}{mn\gamma_i}\right)^{-2}, \tag{12}$$

and γ_i denotes the average received SNR at the ith SU. It is worth noting that γ_i varies considering the homogeneous PPP model in this paper and the corresponding closed-form expression is derived as Eq. (20) in Section III-C.

Proof: The proof is provided in the Appendix C. ■

Meanwhile, we derive the analytical expression for calculating the decision threshold in terms of the individual probability of detection seen at the ith SU, which is given by (13) at the top of this page, where the coefficient $C_t = 1$ for $t = 0$ and $C_t = \sum_{q=0}^{t-1}\frac{C_qC_{t-1-q}}{(q+1)(2q+1)}$ for otherwise.

B. Cooperative sensing with reporting errors

In the cooperative spectrum sensing system, the final decision on the status of the PU can be made through different techniques, including decision fusion and data fusion. In this work, we apply decision fusion to investigate the performance of the system. During a decision fusion process, each SU processes the data individually and makes a local decision that is represented by a single bit ($1/0$ represents the presence/absence of the PU) independently. Then, the final decision is made by fusing these individual decisions through a voting rule. Due to the imperfection of the reporting channel between the SUs and the FC, the reporting error may occur during the decision reporting frame of the spectrum sensing process [34]. Assuming the reporting channel bit error probability (BEP) under $\mathcal{H}_0$ and $\mathcal{H}_1$ are represented by $P_{\mathrm{b},i}^0$ and $P_{\mathrm{b},i}^1$ for the ith reporting channel, the probability of false alarm of the ith SU seen at the FC $P_{\mathrm{fa},i}$ with the presence of reporting errors is given by

$$\begin{aligned}P_{\mathrm{fa},i} &= \mathbf{P}\left(u_i^{\mathrm{fc}}=1 \mid \mathcal{H}_0\right)\\ &= \mathbf{P}\left(u_i^{\mathrm{fc}}=1 \mid u_i^{\mathrm{su}}=1\right)\mathbf{P}\left(u_i^{\mathrm{su}}=1 \mid \mathcal{H}_0\right)\\ &+ \mathbf{P}\left(u_i^{\mathrm{fc}}=1 \mid u_i^{\mathrm{su}}=0\right)\mathbf{P}\left(u_i^{\mathrm{su}}=0 \mid \mathcal{H}_0\right)\\ &= (1-P_{\mathrm{b},i}^0)P_{\mathrm{fa},i}^{\mathrm{su}}+P_{\mathrm{b},i}^0(1-P_{\mathrm{fa},i}^{\mathrm{su}}),\end{aligned} \tag{14}$$

where u_i^{fc} and u_i^{su} denote the decision on the status of the PU made by the ith SU seen at the FC and SU respectively. Similarly, the probability of detection of the ith SU seen at the FC with the presence of reporting errors is given by

$$\begin{aligned}P_{\mathrm{d},i} &= \mathbf{P}\left(u_i^{\mathrm{fc}}=1 \mid \mathcal{H}_1\right)\\ &= \mathbf{P}\left(u_i^{\mathrm{fc}}=1 \mid u_i^{\mathrm{su}}=1\right)\mathbf{P}\left(u_i^{\mathrm{su}}=1 \mid \mathcal{H}_1\right)\\ &+ \mathbf{P}\left(u_i^{\mathrm{fc}}=1 \mid u_i^{\mathrm{su}}=0\right)\mathbf{P}\left(u_i^{\mathrm{su}}=0 \mid \mathcal{H}_1\right)\\ &= (1-P_{\mathrm{b},i}^1)P_{\mathrm{d},i}^{\mathrm{su}}+P_{\mathrm{b},i}^1(1-P_{\mathrm{d},i}^{\mathrm{su}}).\end{aligned} \tag{15}$$

Generally, the BEP depends on the modulation scheme and the SNR or signal-to-interference-and-noise ratio (SINR) between the SU and the FC. In order to confine the interference to the PU caused by the missed detection, the FC has to be far away from the PU in practice. Therefore, $P_{\mathrm{b},i}^0$ and $P_{\mathrm{b},i}^1$ are quite close so that the approximation relation $P_{\mathrm{b},i}^0 = P_{\mathrm{b},i}^1$ can be obtained. Furthermore, the BEPs can be controlled within a very low and similar value for different SUs by applying error rate control techniques, including increasing transmit power, utilizing the diversity in space, time and frequency domains, retransmitting the echoed back information, applying automatic repeat request (ARQ) method and employing forward error correction coding (FECC). Thus, the difference of BEPs between different SUs is quite small after employing appropriate error rate control techniques, so that it has little influence on the sensing error rate of the final decision in practice. Based on these conditions in practice, a simplified and reasonable assumption is the reporting processes of different SUs are independent and the BEPs are identical for different SUs, which indicates that $P_{\mathrm{b},i}^0 = P_{\mathrm{b},i}^1 = P_{\mathrm{b}}$. This approximation would not affect the analyses on sensing and transmission performances in this paper, since the difference of BEPs between different SUs is quite small and has little influence on performances of the system after employing error rate control techniques.

Specifically, voting rules Logic-OR (OR) and Logic-AND (AND) are used in this work in order to find out the optimal number of the collaborating SUs conveniently. Assuming there are k cooperating SUs, the properties of the OR and AND rules

are as follows. (1) OR rule: When at least one local decision among the k local decisions indicates the PU is present, the final decision declares the PU is present. The probabilities of detection and false alarm of the final decision are given by

$$P_{\rm d}=1-\prod_{i=1}^{k}(1-P_{{\rm d},i}),\quad P_{\rm fa}=1-\prod_{i=1}^{k}(1-P_{{\rm fa},i}). \quad (16)$$

(2) AND rule: Only when all local decisions indicate the PU is present, the final decision declares the PU is present. The corresponding probabilities of detection $P_{\rm d}$ and false alarm $P_{\rm fa}$ of the final decision are given by

$$P_{\rm d}=\prod_{i=1}^{k}P_{{\rm d},i},\quad P_{\rm fa}=\prod_{i=1}^{k}P_{{\rm fa},i}. \quad (17)$$

The total error rate of the final decision is defined to be the summation of the false alarm and missed detection rates of the final decision, which is given by

$$P_{\rm te}=P_{\rm fa}+P_{\rm m}, \quad (18)$$

where the probability of missed detection of the final decision $P_{\rm m}$ is defined as $P_{\rm m}=1-P_{\rm d}$.

C. Optimal Number of Cooperating SUs

The optimization of the cooperative spectrum sensing can be considered from three perspectives. Firstly, it can be considered under the CDR requirement, which aims to minimize the probability of false alarm for a given probability of detection. This guarantees the benefits of PU preferentially. Secondly, the probability of detection can be minimized for a desired CFAR, which gives priority to the interests of the SUs. Thirdly, this issue can be considered to minimize the total error rate for a given CDT, which considers the interests of PU and SUs concurrently. In this work, the optimization of cooperative spectrum sensing is investigated only under the CDT requirement, however all the expressions and the techniques proposed in this paper can also be applied to the CDR and CFAR cases.

Under the CDT requirement, the decision threshold is fixed and identical for every individual spectrum sensing period. Therefore, the individual probability of false alarm $P_{{\rm fa},i}$ for each SU is constant. However, the individual probability of detection varies depending on γ_i. From (10), it can be found that a higher received SNR helps to achieve a higher individual probability of detection $P_{{\rm d},i}$. Therefore, the SUs with higher received SNRs should be chosen first to implement the cooperative spectrum sensing. In order to study the received SNR at the ith nearest SU, the Euclidean distance d_i between the PU and the ith nearest SU within the coverage radius of FC (shown as Fig. 1) needs to be investigated. The PDF of d_i is derived as the following theorem.

Theorem 3: In a PPP with density ρ on a 2-dimensional plane, the PDF of the distance d_i between the ith nearest SU within the coverage radius of FC from the PU and the PU outside the region of interest is given by

$$f_{d_i}(d)=\frac{2\rho\theta(D-R)e^{-2\rho\theta(D-R)(d-D+R)}}{\Gamma(i)\big(2\rho\theta(D-R)(d-D+R)\big)^{1-i}}, \quad (19)$$

where $\theta=\sin^{-1}\left(\frac{R}{D}\right)$ and $D\gg R$.

Proof: The proof is provided in the Appendix D. ■

Hence, the average received SNR γ_i at the ith nearest SU can be derived as

$$\begin{aligned}\gamma_i&=\int_{D-R}^{\infty}\int_{0}^{\infty}\frac{P_{\rm T}\omega}{\sigma_v^2 d^{\varepsilon}}f_{\omega_i}(\omega)f_{d_i}(d)\quad {\rm d}\omega{\rm d}d\\&=\frac{P_{\rm T}me^{2\rho\theta(D-R)^2}}{\sigma_v^2\big(2\rho\theta(D-R)\big)^{-\varepsilon}}\sum_{j=0}^{i-1}\binom{i-1}{j}\frac{\Gamma\left(i-j-\varepsilon,2\rho\theta(D-R)^2\right)}{\Gamma(i)\left(-2\rho\theta(D-R)^2\right)^{-j}},\end{aligned} \quad (20)$$

where $\Gamma(\cdot,\cdot)$ denotes the upper incomplete Gamma function. Therefore, by using the above result, $P_{{\rm fa},i}$ and $P_{{\rm d},i}$ can be computed under the CDT requirement. Also, the total error rate $P_{\rm te}$ can be obtained under specific decision fusion rules.

According to the above expression of the received SNR measured at the ith nearest SU under the homogeneous PPP model, the received SNR decreases with the increasing i. With the increase of the number of the SUs involved in the cooperative sensing k, the local decision made by the SU with very low received SNR may be included in the final decision so that the sensing performance would be affected. Thus, there exists an optimal number of cooperating SUs $k_{\rm opt}$ that can minimize the total error rate of the final decision. Meanwhile, the decision threshold is predetermined under the CDT requirement. Therefore, the optimization issue can be formulated as follow:

$$k_{\rm opt}=\arg\min_{k}P_{\rm te}(k). \quad (21)$$

Since the total number of available SUs follows Poisson distribution, the optimal solution $k_{\rm opt}$ is difficult to obtain. Therefore, the exhaustive search approach is applied in our work to find the solution to the above optimization issue.

There exist many benefits when cooperating $k_{\rm opt}$ SUs to perform spectrum sensing rather than collaborating all the available SUs all the time. Specifically, firstly, only cooperating a few, not all, the SUs to implement spectrum sensing, the sensing performance (i.e., the total error rate of the final decision in this paper) will be improved which can be seen from the Fig. 4. Secondly, comparing with the traditional approach, less cooperating SUs brings less energy consumption since the unemployed SUs are silent during the sensing and reporting durations. Finally, it is obvious that less cooperating SUs can reduce the reporting time in the time division mode so that the spectrum sensing process can be accelerated. Therefore, for a fixed periodic spectrum sensing frame, the SUs can have more time for data transmission and the achievable ergodic capacity or throughput of the secondary network can be enhanced.

Under the CDT requirement, when an additional SU is added into the cooperative spectrum sensing, the additional SU has the worst individual probability of detection, i.e. $P_{{\rm d},k}$, among the cooperating SUs. However, the individual probability of false alarm of the additional SU $P_{{\rm fa},k}$ is identical with other cooperating SUs. Meanwhile, the additional SU does not affect the performance of the other SUs.

1) OR rule: The total error rate of the final decision $P_{\rm te}$ under OR rule can be given by

$$P_{\rm te}=1-\prod_{i=1}^{k}(1-P_{{\rm fa},i})+\prod_{i=1}^{k}(1-P_{{\rm d},i}). \quad (22)$$

Because of the properties of $P_{\mathrm{fa},i}$ and $P_{\mathrm{m},i}$ mentioned above, it can be seen from (16) that the probability of false alarm of the final decision P_{fa} increases with the increase of the cooperating SUs' number k, but the probability of missed detection of the final decision P_{m} falls down. Due to the monotonicity of P_{m} and P_{fa}, it can be seen from (18) that collaborating all the SUs in the secondary network is not always the best option. The performance of the total error rate is determined by the absolute values of the slope of P_{fa} and P_{m} with the increase of k. Therefore, under two cases, collaborating all the available SUs may not achieve the minimum total error rate. Firstly, when the absolute values of the slope of P_{fa} and P_{m} are similar, the total error rate of the final decision will reduce initially and rise later with the increase of k. Secondly, when the absolute value of the slope of P_{fa} is larger than the value of P_{m}, the total error rate increases with the increasing k. By utilizing (5), (10) and (22), the total error rate can be calculated and the optimal number of the cooperating SUs k_{opt} can be obtained.

2) AND rule: Under the AND rule, the total error rate is given by

$$P_{\mathrm{te}} = 1 - \prod_{i=1}^{k} P_{\mathrm{d},i} + \prod_{i=1}^{k} P_{\mathrm{fa},i}. \tag{23}$$

Compared with the OR rule, it can be seen from (17) that P_{fa} is a decreasing function and P_{m} is an increasing function with regard to the number of the cooperating SUs k under the AND rule. From (18), the trend of the total error rate of the final decision is also decided by the absolute values of the slope of P_{fa} and P_{m}. Hence, collaborating all the SUs in the network may not guarantee that the total error rate achieves the minimum value. By utilizing (5), (10) and (23), the total error rate when using AND rule under CDT requirement can be computed and the optimal number of the SUs can be obtained when the number of available SUs is large.

Remark 1: Nowadays, there exists many wideband signals in practical applications, eg. the orthogonal-frequency-division-multiplexing (OFDM) encoding signals, multi-tone transmit signals and signals over consecutive block-fading channels. The spectrum sensing techniques for these wideband signals have been proposed and studied in literatures, such as using the variational message passing algorithm or wavelet transform to estimate the power spectral density of wideband signals. However, the results shown in this paper are still valid for wideband spectrum sensing, when the subchannel is sensed in a sequential manner. One potential solution is the radio frequency front-end is equipped with a tunable narrowband bandpass filter [35]. So one narrow frequency band can be searched at a time and existing narrowband spectrum sensing techniques can be applied. This is a way to extend our current work to a practical system with wideband primary signals.

IV. Achievable ergodic capacity and throughput

In this section, the achievable ergodic capacity and throughput of the CR network are investigated in order to capture the performance of the sensing-based secondary links. As shown in Fig. 1, the RRHs are the secondary transmitters (SU-Txs) and the secondary receiver (SU-Rx) is located at the origin of the secondary network region. As agreed in the section II, each SU-Tx is equipped with multiple antennas and the SU-Rx is with single antenna. The path loss and Rayleigh fading between the SU-Tx and SU-Rx are considered in this paper. When the PU is absent, the received SNR at the SU-Rx sourced from each SU-Tx is given as

$$\gamma^{\mathrm{s0}} = \frac{P_{\mathrm{ST}}}{L^{\varepsilon}\sigma^2}\alpha, \tag{24}$$

where P_{ST} denotes the transmitted signal power from the SU-Tx, σ^2 is the additive noise power at the SU-Rx, L is the distance between each SU-Tx and SU-Rx, ε is the path loss factor and α denotes the Rayleigh fading channel gain in each secondary link. When the maximal ratio transmission (MRT) is applied, the PDF of α is given as

$$f_{\alpha}(\alpha) = \frac{\alpha^{m-1}e^{-\alpha}}{(m-1)!}, \tag{25}$$

and the PDF of L is given by

$$f_{L}(L) = \frac{2L}{R^2}. \tag{26}$$

Meanwhile, when the PU is present, the interference from the PU's signal is considered and the received signal-to-inference-plus-noise ratio (SINR) is given by

$$\gamma^{\mathrm{s1}} = \frac{P_{\mathrm{ST}}L^{-\varepsilon}\alpha}{\sigma^2 + P_{\mathrm{T}}D^{-\varepsilon}\beta}, \tag{27}$$

where β denotes the Rayleigh fading gain between the PU and the SU-Rx and β follows the exponential distribution with mean 1, i.e.,

$$f_{\beta}(\beta) = \exp(-\beta). \tag{28}$$

For a CR network, one periodic spectrum sensing frame T_{f} consists of three parts, including the sensing slot T_{s}, decision reporting slot T_{r} and data transmission slot T_{t}. In the interweave method, the data transmission of the secondary links can be carried out under two situations, one is there is no false alarm when the PU is absent and the other one is missed detection occurs when the PU is present. Therefore, the achievable ergodic capacity and throughput of the secondary network are also comprised of these two parts.

A. Achievable Ergodic Capacity

Based on the structure of the CR system mentioned above, the achievable capacity of each secondary link in the CR system can be given by

$$C_{\mathrm{ac}} = C_{\mathrm{ac0}} + C_{\mathrm{ac1}}, \tag{29}$$

where C_{ac0} denotes the achievable capacity with the absence of the PU and C_{ac1} denotes the achievable capacity with the presence of the PU. Specifically, C_{ac0} and C_{ac1} can be obtained as follows

$$C_{\mathrm{ac0}} = \left(\frac{T_{\mathrm{f}} - T_{\mathrm{s}} - kT_{\mathrm{r}}}{T_{\mathrm{f}}}\right)\log_2(1+\gamma^{\mathrm{s0}})(1-P_{\mathrm{fa}})P(\mathcal{H}_0), \tag{30}$$

$$C_{\mathrm{ac1}} = \left(\frac{T_{\mathrm{f}} - T_{\mathrm{s}} - kT_{\mathrm{r}}}{T_{\mathrm{f}}}\right)\log_2(1+\gamma^{\mathrm{s1}})(1-P_{\mathrm{d}})P(\mathcal{H}_1), \tag{31}$$

where k is the number of the SUs involved in the cooperative sensing, $P(\mathcal{H}_0)$ and $P(\mathcal{H}_1)$ represent the probabilities that the PU is absent and present respectively.

1) Achievable ergodic capacity under $\mathcal{H}_0$:

Proposition 1: The achievable ergodic capacity of each secondary link when the PU is absent can be derived as

$$\overline{C_{\rm ac0}} = \frac{2G_{4,3}^{2,3}\left(\frac{P_{\rm ST}R^{-\varepsilon}}{\sigma^2}\middle|\begin{matrix}1-m,1,1,\frac{2}{\varepsilon}+1\\ \frac{2}{\varepsilon},1,0\end{matrix}\right)}{\varepsilon(m-1)!\ln(2)} \times\left(\frac{T_{\rm f}-T_{\rm s}-kT_{\rm r}}{T_{\rm f}}\right)(1-P_{\rm fa})P(\mathcal{H}_0). \quad (32)$$

Proof: In order to derive the expression of $\overline{C_{\rm ac0}}$, we first obtain the statistical average of $\log_2(1+\gamma^{\rm s0})$. Let $C_{\rm ec0}=\log_2(1+\gamma^{\rm s0})$ and the statistical average $\overline{C_{\rm ec0}}$ can be calculated by

$$\overline{C_{\rm ec0}} = \int_0^R\int_0^\infty \log_2\left(1+\frac{P_{\rm ST}}{L^\varepsilon\sigma^2}\alpha\right) f_\alpha(\alpha)f_L(L){\rm d}\alpha{\rm d}L = \int_0^R\int_0^\infty \frac{\ln\left(1+\frac{P_{\rm ST}}{L^\varepsilon\sigma^2}\alpha\right)}{\ln(2)}\frac{\alpha^{m-1}e^{-\alpha}}{(m-1)!}\frac{2L}{R^2}{\rm d}\alpha{\rm d}L. \quad (33)$$

By utilizing the equality relationship $\ln(1+ax)=G_{2,2}^{1,2}\left(ax\middle|\begin{matrix}1,1\\1,0\end{matrix}\right)$, the calculation of $\overline{C_{\rm ec0}}$ can be rewritten as

$$\overline{C_{\rm ec0}} = \int_0^R\int_0^\infty G_{2,2}^{1,2}\left(\frac{P_{\rm ST}\alpha}{\sigma^2L^\varepsilon}\middle|\begin{matrix}1,1\\1,0\end{matrix}\right)\frac{\alpha^{m-1}}{e^\alpha}{\rm d}\alpha\frac{2L/\ln(2)}{R^2(m-1)!}{\rm d}L = \int_0^R G_{3,2}^{1,3}\left(\frac{P_{\rm ST}}{\sigma^2L^\varepsilon}\middle|\begin{matrix}1-m,1,1\\1,0\end{matrix}\right)\frac{2L/\ln(2)}{(m-1)!R^2}{\rm d}L. \quad (34)$$

Let $z=\left(\frac{R}{L}\right)^\varepsilon$, the equation above can be reorganized. After further manipulations with the aid of [32, (7.811.3)], the expression of $\overline{C_{\rm ec0}}$ can be derived and the expression (32) can be achieved. ∎

2) Achievable ergodic capacity under $\mathcal{H}_1$: The achievable ergodic capacity of each secondary link when the PU is present can be derived as

$$\begin{aligned}\overline{C_{\rm ac1}} &= (1-P_{\rm d})P(\mathcal{H}_1)\int_0^\infty\int_0^R\int_0^\infty \log_2\left(1+\frac{P_{\rm ST}L^{-\varepsilon}\alpha}{\sigma^2+P_{\rm T}D^{-\varepsilon}\beta}\right) \times f_\alpha(\alpha)f_L(L)f_\beta(\beta){\rm d}\alpha{\rm d}L{\rm d}\beta\\ &=\int_0^\infty \frac{2G_{4,3}^{2,3}\left(\frac{P_{\rm ST}R^{-\varepsilon}}{\sigma^2+P_{\rm T}D^{-\varepsilon}\beta}\middle|\begin{matrix}1-m,1,1,\frac{2}{\varepsilon}+1\\ \frac{2}{\varepsilon},1,0\end{matrix}\right)}{\varepsilon(m-1)!\ln(2)}e^{-\beta}{\rm d}\beta \times\left(\frac{T_{\rm f}-T_{\rm s}-kT_{\rm r}}{T_{\rm f}}\right)(1-P_{\rm d})P(\mathcal{H}_1). \quad (35)\end{aligned}$$

By utilizing the expressions (32) and (35), the achievable ergodic capacity of each secondary link $\overline{C_{\rm ac}}$ can be obtained by

$$\overline{C_{\rm ac}} = \overline{C_{\rm ac0}} + \overline{C_{\rm ac1}}. \quad (36)$$

Therefore, considering all the secondary links, the achievable ergodic capacity of the secondary network[1] based on the homogeneous PPP is given by

$$\overline{C_{\rm c}} = \sum_{N=1}^\infty N\overline{C_{\rm ac}}\mathbf{P}\{N \text{ SU-Txs within secondary network}\} = \sum_{N=1}^\infty \overline{C_{\rm ac}}e^{-4\rho\theta DR}\frac{(4\rho\theta DR)^N}{(N-1)!}. \quad (37)$$

[1]In this paper, the achievable ergodic capacity of the secondary network means the summation of the achievable ergodic capacity of all the available secondary links. Similarly, the achievable throughput of the secondary network is defined in the same way.

The value of $\overline{C_{\rm c}}$ converges with the increasing N, since the probability that there exists N secondary links approaches 0 with the increase of N.

B. Achievable Throughput

Similarly, the achievable throughput $C_{\rm at}$ of each secondary link can be defined as

$$C_{\rm at} = C_{\rm at0} + C_{\rm at1}, \quad (38)$$

where $C_{\rm at0}$ and $C_{\rm at1}$ denote the achievable throughput of each secondary link when the PU is absent and present respectively. In detail, $C_{\rm at0}$ and $C_{\rm at1}$ can be calculated as

$$C_{\rm at0}=\left(\frac{T_{\rm f}-T_{\rm s}-kT_{\rm r}}{T_{\rm f}}\right)\log_2(1+T)P_{\rm cov0}(1-P_{\rm fa})P(\mathcal{H}_0), \quad (39)$$

$$C_{\rm at1}=\left(\frac{T_{\rm f}-T_{\rm s}-kT_{\rm r}}{T_{\rm f}}\right)\log_2(1+T)P_{\rm cov1}(1-P_{\rm d})P(\mathcal{H}_1), \quad (40)$$

where the coverage probabilities $P_{\rm cov0}$ and $P_{\rm cov1}$ are defined as the probability that the received SNR or SINR at the SU-Rx is larger than the preset threshold T when the PU is absent and present respectively.

1) Achievable throughput under $\mathcal{H}_0$:

Proposition 2: The coverage probability $P_{\rm cov0}$ achieved by each secondary link when the PU is absent, i.e. under the hypothesis $\mathcal{H}_0$, can be derived as

$$P_{\rm cov0} = \sum_{t=0}^{m-1}\frac{2T^{-\frac{2}{\varepsilon}}\left(\frac{P_{\rm ST}}{\sigma^2}\right)^{\frac{2}{\varepsilon}}}{\varepsilon R^2t!}\gamma\left(t+\frac{2}{\varepsilon},\frac{T\sigma^2}{P_{\rm ST}}R^\varepsilon\right), \quad (41)$$

where $\gamma(\cdot,\cdot)$ denotes the lower incomplete Gamma function.

Proof: According to the definition of the coverage probability, the coverage probability under the hypothesis $\mathcal{H}_0$ can be written as

$$\begin{aligned}P_{\rm cov0} &= \Pr[\gamma^{\rm s0}\ge T] = \mathbb{E}\left[\Pr\left[\alpha\ge T\frac{L^\varepsilon\sigma^2}{P_{\rm ST}}\right]\middle| L\right]\\ &= \mathbb{E}\left[\frac{\Gamma\left(m,\frac{T\sigma^2}{P_{\rm ST}}L^\varepsilon\right)}{(m-1)!}\middle| L\right]\\ &= \int_0^R\sum_{t=0}^{m-1}\exp\left(-\frac{T\sigma^2}{P_{\rm ST}}L^\varepsilon\right)L^{\varepsilon t}\frac{T^t\sigma^{2t}}{{P_{\rm ST}}^t t!}\frac{2L}{R^2}{\rm d}L, \quad (42)\end{aligned}$$

by utilizing the definition of the lower incomplete Gamma function and after further manipulations, the closed-form expression of the coverage probability under the hypothesis $\mathcal{H}_0$ can be obtained as equation (41). ∎

Therefore, the closed-form expression of the achievable throughput for each secondary link under the hypothesis $\mathcal{H}_0$ can be obtained by utilizing equation (39) and (41).

2) Achievable throughput under $\mathcal{H}_1$:

Proposition 3: When the PU is present, the interference to the secondary network sourced from the PU is considered. The coverage probability of each secondary link under the hypothesis $\mathcal{H}_1$ is derived as

$$P_{\rm cov1}=\sum_{t=0}^{m-1}\sum_{w=0}^{\infty}\frac{2(-1)^wR^{\varepsilon(t+w)}e^{\frac{\sigma^2D^\varepsilon}{P_{\rm T}}}\Gamma\left(t+w+1,\frac{\sigma^2D^\varepsilon}{P_{\rm T}}\right)}{\varepsilon t!w!\left(t+w+\frac{2}{\varepsilon}\right)(P_{\rm T}D^{-\varepsilon}T/P_{\rm ST})^{-t-w}}. \quad (43)$$

Proof: Based on the definition of the coverage probability, the coverage probability under the hypothesis $\mathcal{H}_1$ can be calculated as

$$\begin{aligned} P_{\text{cov1}} &= \Pr[\gamma^{\text{s1}} \geq T] \\ &= \mathbb{E}\left[\Pr\left[\alpha \geq \frac{\sigma^2 + P_{\text{T}} D^{-\varepsilon}\beta}{P_{\text{ST}} L^{-\varepsilon}} T\right] \middle| \beta, L\right] \\ &= \mathbb{E}\left[\frac{\Gamma\left(m, \frac{T(\sigma^2+P_{\text{T}}D^{-\varepsilon}\beta)}{P_{\text{ST}}} L^{\varepsilon}\right)}{\Gamma(m)} \middle| \beta, L\right] \\ &= \int_0^{\infty} \sum_{t=0}^{m-1} \frac{2\gamma\left(t+\frac{2}{\varepsilon}, \frac{TR^{\varepsilon}}{P_{\text{ST}}}(\sigma^2+P_{\text{T}}D^{-\varepsilon}\beta)\right)}{\varepsilon t! R^2 e^{\beta}\left(\frac{P_{\text{ST}}/T}{\sigma^2+P_{\text{T}}D^{-\varepsilon}\beta}\right)^{-\frac{2}{\varepsilon}}} \mathrm{d}\beta, \quad (44) \end{aligned}$$

By defining $z = \frac{T}{P_{\text{ST}}}(\sigma^2 + P_{\text{T}} D^{-\varepsilon}\beta)$ and utilizing the power series expansion of the lower incomplete Gamma function, the integral above can be rewritten as

$$P_{\text{cov1}} = \int_{\frac{T\sigma^2}{P_{\text{ST}}}}^{\infty} \sum_{t=0}^{m-1} \sum_{w=0}^{\infty} \frac{2D^{\varepsilon} P_{\text{ST}} R^{\varepsilon(t+w+\frac{2}{\varepsilon})} e^{\frac{T\sigma^2 - z P_{\text{ST}}}{P_{\text{T}} D^{-\varepsilon} T}} z^{t+w}}{(-1)^{-w} P_{\text{T}} T \varepsilon t! w! R^2 (t+w+\frac{2}{\varepsilon})} \mathrm{d}z.$$

The above integral can be calculated with the aid of the definition of the upper incomplete Gamma function and then the expression of (43) can be arrived. ∎

By using the equation (40) and the expression (43), the achievable throughput of each secondary link can be obtained under the presence of the PU.

After the expressions of the coverage probability under the hypothesis $\mathcal{H}_0$ and $\mathcal{H}_1$ are derived, the closed-form expressions of the achievable throughput when the PU is absent and present can be obtained by utilizing (39) and (40). Therefore, the achievable throughput C_{at} of each secondary link can be obtained by using (38).

Furthermore, considering all the available secondary links, the achievable throughput of the secondary network based on the homogeneous PPP is given by

$$\begin{aligned} C_{\text{th}} &= \sum_{N=1}^{\infty} N C_{\text{at}} \mathbf{P}\{N \text{ SU-Txs within secondary network}\} \\ &= \sum_{N=1}^{\infty} C_{\text{at}} e^{-4\rho\theta DR} \frac{(4\rho\theta DR)^N}{(N-1)!}. \quad (45) \end{aligned}$$

It is worth mentioning that the value of C_{th} converges with the increase of N, since the probability of having N secondary links approaches 0 when N is large enough.

V. Simulation Results And Discussions

In this section, simulation results are provided to validate the derived expressions and the analyses throughout this paper. In the simulation results, it is assumed that the coverage radius of the FC is $R = 5$ km, the distance between the FC and PU is $D = 50$ km. The transmit power of PU is 5 W, the additive noise power is -90 dBm. The path loss exponent factor is $\varepsilon = 3.1$. When employing binary phase-shift keying (BPSK) modulation scheme and error rate control methods, the BEP during the decision reporting process is assumed as $P_{\text{b}} = 10^{-2}$. The sampling frequency of the signal $f_{\text{s}} = 6$ MHz, the data rate of the reporting channel $R_{\text{b}} = 100$ Kbps so that $T_{\text{r}} = \frac{1}{R_{\text{b}}}$. One periodic frame of the SU is $T_{\text{f}} = 100$ ms and the density in the considered PPP is $\rho = 10^{-7}$ nodes/m^2.

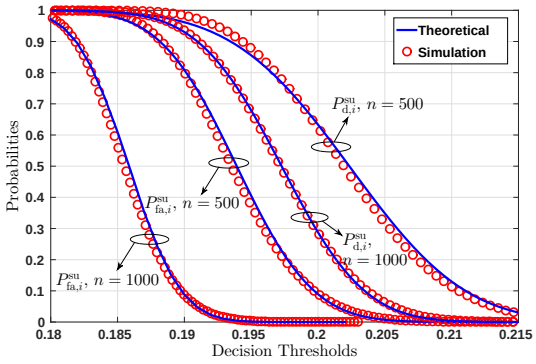

Fig. 2. The individual probabilities of false alarm and detection seen at ith SU versus decision thresholds for various sample size n, the number of receive antennas for each SU is $m = 6$ and the received SNR $= -15$ dB

Fig. 2 verifies the generalized expressions of the individual probabilities of false alarm and detection seen at the ith SU. Assuming each SU is equipped with 6 receive antennas, i.e., m = 6, the analytical and Monte-Carlo results of $P_{\text{fa},i}$ and $P_{\text{d},i}$ are plotted for various cases of the received signal sample size n = $\{500, 1000\}$. Besides, $P_{\text{d},i}$ is plotted under the received SNR = -15 dB. It can be observed that the analytical results match the Monte-Carlo simulations even under very low received SNR. Fig. 3 validates the expression of the PDF of the distance between the ith nearest SU and the PU derived as (19) in this paper. This figure represents the PDF of the Euclidean distance of the second and fourth nearest SU from the PU. It can be seen that the analytical results match with the Monte-Carlo results very well, which proves that the closed-form expression of the distance between the PU and its ith nearest neighbour located within the area of interest.

Fig. 4 depicts the total error rate of the final decision versus the number of collaborating SUs under the CDT requirement by using OR and AND fusion rules, respectively. Due to the verifications in Fig. 2 and Fig. 3, only the analytical results are shown in this figure. In this figure, the preset decision threshold is 0.28, each SU is assumed with 4 receive antennas ($m = 4$) and the sample size of received signal is $n = \{600, 800\}$. The total error rate of the final decision can be calculated as described in Section III. Since the number of available SUs in PPP is random, it is impossible to show all the possible cases of different number of SUs. However, The probability of above certain number of SUs within the coverage radius of FC can be calculated by using (55). For the PPP with the determined density ρ considered in this paper, the probability of over 14 SUs located within the area of interest is under 0.05. Thus, Fig. 4 only shows the case of the number of available SUs up to 14, which is enough for analysis. It can be seen that the total error rate decreases first and then increases with the increase of the number of cooperating SUs, under the AND rule. The optimal numbers of cooperating SUs are $k_{\text{opt}} = \{3, 2\}$ which makes the total error rates achieve the minimum values $\{0.07, 0.03\}$ for the cases of $n = \{600, 800\}$, respectively. Under the OR rule, the total error rate increases with the increasing k. Hence, single node spectrum sensing based on the nearest SU can achieve the best sensing performance. Therefore, it can be deduced that cooperating all the available SUs is not always

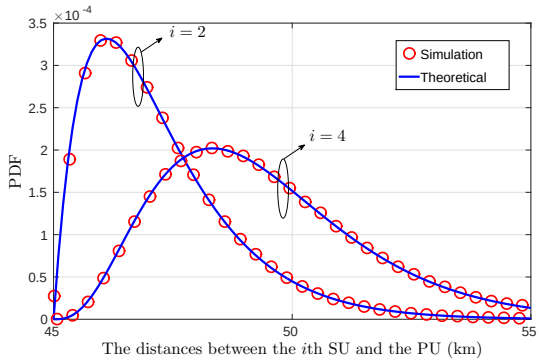

Fig. 3. The PDF of the distances between the ith SU within the area of interest and the PU

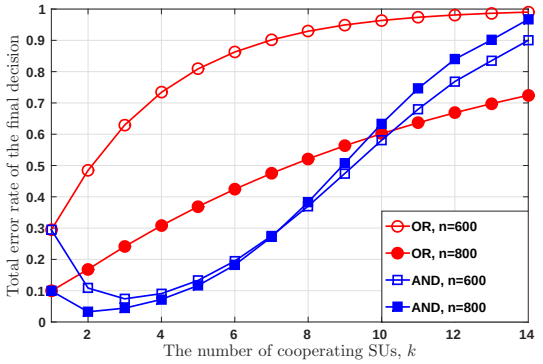

Fig. 4. The total error rate of the final decision versus the number of cooperating SUs k for various sample size n by using OR and AND fusion rules under the CDT requirement

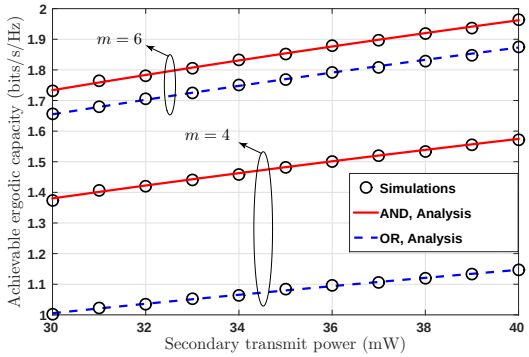

Fig. 5. The achievable ergodic capacity versus the secondary transmit power under different fusion rules, the antenna number at each SU-Tx is $m = 4, 6$ and the sample size is $n = 600$

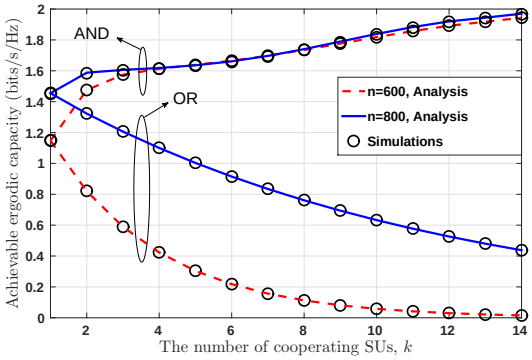

Fig. 6. The achievable ergodic capacity versus the number of cooperating SUs under different fusion rules, each SU-Tx is with 4 antennas and the sample size is $n = 600, 800$

necessary to achieve the best sensing performance. When the SUs follow a homogeneous PPP and the number of available SUs is large, cooperating k_{opt} SUs (not always all the SUs) not only improves the accuracy of spectrum sensing, but also accelerates the cooperative spectrum sensing.

Fig. 5 shows the achievable ergodic capacity of each secondary link versus the transmit power of the SU-Tx from 30 mW to 40 mW under the CDT requirement when achieving the minimum total error rate. The minimum total error rate can be obtained by utilizing the method proposed in section III. In this figure, various cases are presented under different numbers of SU-Tx antennas (i.e., $m = 4$, $m = 6$) and different decision fusion rules. Besides, the sample number of the PU's signal is $n = 600$. Under the CDT requirement, a preset decision threshold is required. The definition area of the decision threshold is $[1/m, 1]$, which means the definition area of the decision thresholds can vary depending on the number of antennas at each SU-Tx. Therefore, the predefined decision thresholds are assumed to be 0.28 and 0.24 for the cases of $m = 4$ and $m = 6$ respectively. Furthermore, it can be seen that the achievable ergodic capacity of the secondary network rises monotonously with the increasing transmit power of the secondary transmitter. When comparing the achievable ergodic capacity in terms of decision fusion rules, the AND rule outperforms the OR rule for a same number of SU-Tx antennas. Besides, it can be seen that the gap of the achievable ergodic capacity between the AND and OR fusion rules reduces with increasing m.

Fig. 6 represents the achievable ergodic capacity of each secondary link versus the number of the cooperating SUs under the CDT requirement when the SUs follows a PPP with density ρ. In this figure, each SU-Tx is equipped with 4 antennas and the sample number of the PU's signal is $n = 600, 800$. The predefined decision threshold is 0.28 and the transmit power of the secondary transmitter is $P_{\text{ST}} = 40$ mW. The other parameter setting is same with the previous part. Firstly, the achievable ergodic capacity by using the AND decision fusion rule is higher than the results by using the OR rule when each SU-Tx is with the same number of antennas. Secondly, it can also be seen that a larger sample number of the PU's signal can help to improve the achievable ergodic capacity of the secondary network. Furthermore, when the AND fusion rule is applied, the achievable ergodic capacity increases with increasing k. However, under the OR fusion rule, the achievable ergodic capacity decreases with increasing k. Under the CDT requirement, for the AND decision fusion rule, both P_{fa} and P_{d} are decreasing functions with regard to k. However, when the OR fusion rule is applied, P_{fa} and P_{d} both increase with the increasing k. Thus, for given primary and secondary transmit powers, it can be found from (29), (30) and (31) that the achievable ergodic capacity of the secondary network increases under the AND rule and decreases under the OR rule with the increase of k. Therefore, considering the total error rate of the final decision performance shown as Fig. 4 and the achievable ergodic capacity described in Fig. 6 together, the method of choosing the optimum number of cooperating SUs should be as follows:

In order to achieve a high achievable ergodic capacity and an acceptable total error rate concurrently, the eligible numbers

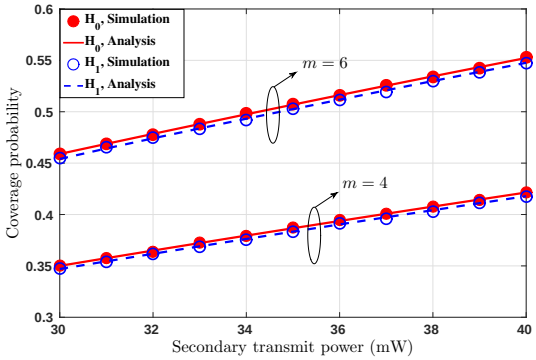

Fig. 7. The coverage probability versus the secondary transmit power under the hypothesis $\mathcal{H}_0$ and $\mathcal{H}_1$, the antenna number at each SU-Tx is $m = 4, 6$

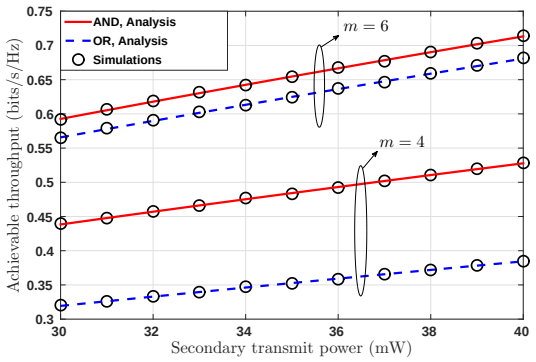

Fig. 8. The achievable throughput versus the secondary transmit power under different fusion rules, the antenna number at each SU-Tx is $m = 4, 6$ and the sample size is $n = 600$

of the cooperating SUs can be determined first for a target total error rate and then the optimum number of cooperating SUs which maximizes the achievable ergodic capacity can be selected among the eligible numbers obtained. Specifically, the achievable ergodic capacity is an increasing function with regard to k for the AND rule, but it is a decreasing function for the OR rule. Hence the largest number of the cooperating SUs which satisfies the desired total error rate requirement should be chosen to maximize the achievable ergodic capacity for the AND rule. On the contrary, the smallest number of the collaborating SUs that makes the total error rate under or equal to the targeted value is selected for the OR rule.

Fig. 7 describes the coverage probability of each secondary link versus the transmit power of the secondary transmitter from 30 mW to 40 mW under the hypotheses $\mathcal{H}_0$ and $\mathcal{H}_1$. The predefined threshold of the received SNR and SINR at the secondary receiver is assumed to be 3 dB. Two cases (i.e., $m = 4, m = 6$) are presented in this figure under the hypotheses $\mathcal{H}_0$ and $\mathcal{H}_1$ respectively. From this figure, the coverage probabilities under the hypotheses $\mathcal{H}_0$ and $\mathcal{H}_1$ both increase with the increasing secondary transmit power. Furthermore, it can also be observed that more antennas at each SU-Tx help to improve the coverage probability, which can also be inferred from the expressions (41) and (43).

Fig. 8 shows the achievable throughput performance of each secondary link with the increase of the secondary transmit power from 30 mW to 40 mW when the minimum total error rate is achieved. Multiple cases are represented for different numbers of antennas at each SU-Tx (i.e., $m = 4, m = 6$) and decision fusion rules. It can be seen that the achievable

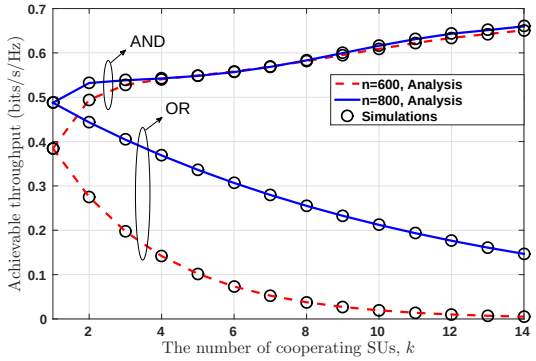

Fig. 9. The achievable throughput versus the number of cooperating SUs under different fusion rules, each SU-Tx is with 4 antennas and the sample size is $n = 600, 800$

throughput increases with the increase of the secondary transmit power and the number of the antennas at each SU-Tx under both of the fusion rules. Besides, the AND fusion rule can achieve a better achievable throughput than the OR rule.

Fig. 9 presents the achievable throughput of each secondary link with the increase of the number of the cooperating SUs under the CDT requirement. The transmit power of the SU-Tx is 40 mW and the preset decision threshold is 0.28. Firstly, for a given sample size, the AND rule can achieve a higher achievable throughput of the secondary network than the OR rule under the CDT requirement. Secondly, a larger sample size helps to obtain a higher achievable throughput of the secondary network. Lastly, the achievable throughput of the secondary network increases with the number of cooperating SUs under the AND rule, however, it decreases with the increasing k under the OR rule. Therefore, considering the total error rate performance and the achievable throughput of the secondary network concurrently, different strategies should be used to determine the optimal number of cooperating SUs for different decision fusion rules. Specifically, under the AND rule, the chosen number of cooperating SUs should be as large as possible while not exceeding the target total error rate. On the contrary, under the OR rule, the chosen number of cooperating SUs should be as small as possible based on the target total error rate requirement.

VI. Conclusions

This paper investigated the efficient cooperative spectrum sensing in CR networks by using the GLRT detector when SUs follow a homogeneous PPP. The analytical expressions of the individual probabilities of false alarm and detection were derived for the general case of the GLRT detector in order to analyze the total error rate performance of the cooperative sensing system. The total error rate of the final decision was then investigated when cooperating different numbers of SUs under OR and AND fusion rules, respectively. It is worth mentioning that reporting errors were also considered in this paper. The analytical results indicated that cooperating all the SUs could not always achieve the best spectrum sensing performance and the obtained optimal numbers of cooperating SUs in this paper minimized the total error rates of the final decisions. It is worth noting that the SUs with higher received SNRs are preferred to implement cooperative spectrum sensing. Besides, the analytical expressions of the

$$f^{(1)}_{\mathrm{GLRT}}(x)=\frac{(m-1)\left(1-\frac{1+m\gamma_i}{mn\gamma_i}\right)}{\sqrt{\frac{2\pi}{n}}(1+m\gamma_i)(1-x)^2}\times\exp\left(-\frac{n}{2}\left[\frac{x(m-1)}{1-x}\left(\frac{1}{1+m\gamma_i}-\frac{1}{mn\gamma_i}\right)-\left(1+\frac{m-1}{mn\gamma_i}\right)\right]^2\right). \quad (53)$$

achievable ergodic capacity and throughput of the secondary network were derived. We also studied the impact of the number of cooperating SUs to conduct spectrum sensing on the achievable ergodic capacity and throughput of the secondary network. Accordingly, different strategies were proposed to determine the optimum number of cooperating SUs in order to achieve the best transmission performances for different fusion rules while not exceeding the target total error rate.

APPENDIX

A. Proof of Theorem 1

The test statistic T_{GLRT} can be rewritten as $T_{\mathrm{GLRT}}=\frac{1}{m}\frac{m\hat{\lambda}_{\max}}{\sum_{l=1}^{m}\hat{\lambda}_l}=x$. Let $z=\frac{m\hat{\lambda}_{\max}}{\sum_{l=1}^{m}\hat{\lambda}_l}$ and $f_z(z)$ denote the PDF of z, therefore $x=g(z)=\frac{z}{m}$ and the PDF of T_{GLRT} can be calculated by $f^{(0)}_{\mathrm{GLRT}}(x)=\left.\frac{f_z(z)}{\left|\frac{\mathrm{d}}{\mathrm{d}z}(g(z))\right|}\right|_{z=mx}$, where the expression of $f_z(z)$ is given in [29]. After further calculations, the expression of the PDF of the test statistic under $\mathcal{H}_0$ can be derived as

$$f^{(0)}_{\mathrm{GLRT}}(x)=\frac{\Gamma(mn)\eta^{1-mn}}{\Gamma(mn-\xi)\Gamma(\xi)}x^{\xi-1}(\eta-x)^{mn-\xi-1}. \quad (46)$$

After solving the integral, the cumulative distribution function (CDF) of the decision threshold under the hypothesis $\mathcal{H}_0$ can be derived and the expression of (5) can be obtained. It is worth mentioning that the parameters a,b,η and ξ are related to the Tracy-Widom distribution of order 2. Specifically, it is known from [36] that $\frac{\hat{\lambda}_{\max}-a}{b}$ converges to the Tracy-Widom distribution of order 2 under $\mathcal{H}_0$, when $m\ll n$ and n is large enough. Therefore, the expectation and variance of $\hat{\lambda}_{\max}$ is given as

$$\mathbb{E}[\hat{\lambda}_{\max}]=a-1.7711b,\quad \mathrm{Var}[\hat{\lambda}_{\max}]=0.8132b^2, \quad (47)$$

where -1.7711 and 0.8132 are the statistical expectation and variance of the Tracy-Widom distribution of order 2. Meanwhile, $\hat{\lambda}_{\max}$ can be approximated well by the Gamma distribution with scale and shape parameters η,ξ so that

$$\mathbb{E}[\hat{\lambda}_{\max}]=\eta\xi,\quad \mathrm{Var}[\hat{\lambda}_{\max}]=\eta^2\xi. \quad (48)$$

By using the equations (47) and (48), the expressions of parameters η and ξ can be obtained.

B. Proof of Eq. (9)

The expression (9) is of significance to the individual and cooperative sensing performance analyses, especially under the CFAR requirement. We aim to solve $P^{\mathrm{su}}_{\mathrm{fa},i}(x)=\epsilon$ given that $\epsilon\in[0,1]$ and $P^{\mathrm{su}}_{\mathrm{fa},i}(x)$ is given in Eq. (5). This is equivalent to finding the value of x that satisfies

$$\begin{aligned}&{}_2F_1\left(\xi,\xi-mn+1;\xi+1;\frac{x}{\eta}\right)(mx)^{\xi}\\&={}_2F_1\left(\xi,\xi-mn+1;\xi+1;\frac{1}{m\eta}\right)\\&\quad+\frac{\xi\Gamma(mn-\xi)\Gamma(\xi)}{\Gamma(mn)(m\eta)^{-\xi}}(1-\epsilon), \quad (49)\end{aligned}$$

which can be rewritten as

$$\begin{aligned}&G^{1,2}_{2,2}\left(\begin{matrix}1-\xi,mn-\xi\\0,-\xi\end{matrix}\,\middle|\,-\frac{x}{\eta}\right)\\&\quad=(mx)^{-\xi}{}_2F_1\left(\xi,\xi-mn+1;\xi+1;\frac{1}{m\eta}\right)\\&\qquad+\xi!(mn)_{-\xi}(1-\epsilon)\left(\frac{\eta}{x}\right)^{\xi}, \quad (50)\end{aligned}$$

which can be expressed as an incomplete beta function, and hence the value of x can be given by the inverse.

C. Proof of Theorem 2

The largest eigenvalue $\hat{\lambda}_{\max}$ of the sample covariance matrix follows a Gaussian distribution [37] under the hypothesis $\mathcal{H}_1$, which is given as

$$\hat{\lambda}_{\max}\sim\mathcal{N}\left(\lambda_{\max}+\frac{(m-1)\lambda_{\max}\sigma_v^2}{n(\lambda_{\max}-\sigma_v^2)},\frac{\lambda^2_{\max}}{n}\right), \quad (51)$$

where $\lambda_{\max}$ is the actual maximum eigenvalue of the actual covariance matrix $\mathbf{R}_{yy}$ under the hypothesis $\mathcal{H}_1$. Since the determinant of the actual covariance matrix $\det(\mathbf{R}_{yy})=(\sigma_v^2)^{m-1}(P_{\mathrm{T}}d^{-\varepsilon}\|\mathbf{h}\|^2+\sigma_v^2)$ and $\lambda_{\max}=\lambda_1>\lambda_2=\lambda_3=\cdots=\lambda_m$, it can be deduced that $\lambda_{\max}=P_{\mathrm{T}}d^{-\varepsilon}\|\mathbf{h}\|^2+\sigma_v^2$.

The summation of the eigenvalues of the sample covariance matrix $\widehat{\mathbf{R}}_{yy}$ excluding the maximum eigenvalue can be approximated as [38]

$$\sum_{l=2}^{m}\hat{\lambda}_l\approx(m-1)\left(\sigma_v^2-\frac{\sigma_v^2\lambda_{\max}}{(\lambda_{\max}-\sigma_v^2)n}\right)=\psi. \quad (52)$$

The test statistic of the GLRT detector can be rewritten as $T_{\mathrm{GLRT}}=\frac{\hat{\lambda}_{\max}}{\sum_{l=1}^{m}\hat{\lambda}_l}=\frac{\hat{\lambda}_{\max}}{\hat{\lambda}_{\max}+\sum_{l=2}^{m}\hat{\lambda}_l}=x$. Thus, it can be obtained that $\hat{\lambda}_{\max}=\frac{x\psi}{1-x}$. Let $\hat{\lambda}_{\max}=z$ and $f_{\hat{\lambda}_{\max}}(z)$ denote the PDF of $\hat{\lambda}_{\max}$, then the generalized PDF of the test statistic T_{GLRT} under $\mathcal{H}_1$ can be derived through $f^{(1)}_{\mathrm{GLRT}}(x)=\left.\frac{f_{\hat{\lambda}_{\max}}(z)}{\left|\frac{\mathrm{d}}{\mathrm{d}z}\left(\frac{z}{z+\psi}\right)\right|}\right|_{z=\frac{x\psi}{1-x}}$, then the expression of the PDF of T_{GLRT} under $\mathcal{H}_1$ can be derived as (53) at the top of this page. After further mathematical manipulations, the generalized expression of the probability of detection of the local decision seen at the ith SU can be derived as (10).

D. Proof of Theorem 3

When the PU is far from the SUs within the coverage radius of FC, the area of the shadowing region S m^2 in the Fig. 1 can be approximated as

$$S=2\pi(D-R)\frac{2\theta}{2\pi}\big(d-(D-R)\big)=2\theta(D-R)(d-D+R). \quad (54)$$

Since in a homogeneous 2-dimensional PPP with density ρ, the probability of having i nodes in a region $\mathcal{A}$ with the area S m^2 is given by

$$\mathbf{P}\{i\ \text{nodes in}\ \mathcal{A}\}=e^{-\rho S}\frac{(\rho S)^i}{i!}. \quad (55)$$

The complementary CDF of d_i can be computed as the probability that there are less than i SUs within the shadowing

$$f_{d_i}(d) = 2\rho\theta(D-R)e^{-\rho 2\theta(D-R)(d-D+R)} \times \left[\sum_{j=0}^{i-1} \frac{\left(\rho 2\theta(D-R)(d-D+R)\right)^j}{j!} - \sum_{j=1}^{i-1} \frac{\left(\rho 2\theta(D-R)(d-D+R)\right)^{j-1}}{(j-1)!}\right], \quad (57)$$

area (as defined in Section II and Fig. 1), which is given by

$$\begin{aligned} P_i &= \mathbf{P}\{0, 1, \cdots, i-1 \text{ nodes between } D\text{–}R \text{ and } d_i\text{–}(D\text{–}R)\} \\ &= \sum_{j=0}^{i-1} e^{-\rho S_j} \frac{(\rho S_j)^j}{j!}, \end{aligned} \quad (56)$$

By utilizing the relationship between the complementary CDF and the PDF $\left(\text{i.e., } f_{d_i}(d) = -\frac{\mathrm{d}P_i}{\mathrm{d}d}\right)$, The PDF of d_i can be derived as (57) at the top of this page. After further manipulations, the expression of (19) can be obtained.

REFERENCES

[1] CEPT-ECC, "ECC report 205: Licensed shared access (LSA)," Feb. 2014.

[2] S. M. Mishra, A. Sahai, and R. W. Broderson, "Cooperative sensing among cognitive radio," *IEEE ICC*, Jun. 2006.

[3] J. Unnikrishnan and V. V. Veeravalli, "Cooperative sensing for primary detection in cognitive radio," *IEEE J. Sel. Topics Signal Process.*, vol. 2, no. 1, pp. 18–27, Feb. 2008.

[4] J. Shen, T. Jiang, S. Liu, and Z. Zhang, "Maximum channel throughput via cooperative spectrum sensing in cognitive radio networks," *IEEE Trans. Wireless Commun.*, vol. 8, no. 10, pp. 5166–5175, Oct. 2009.

[5] S. Xie, Y. Liu, Y. Zhang, and R. Yu, "A parallel cooperative spectrum sensing in cognitive radio networks," *IEEE Trans. Veh. Technol.*, vol. 59, no. 8, pp. 4079–4092, Oct. 2010.

[6] A. Kortun, T. Ratnarajah, M. Sellathurai, C. Zhong, and C. B. Papadias, "On the performance of eigenvalue-based cooperative spectrum sensing for cognitive radio," *IEEE J. Sel. Topics Signal Process.*, vol. 5, no. 1, pp. 49–55, Feb. 2011.

[7] H. Mu and J. K. Tugnait, "Joint soft-decision cooperative spectrum sensing and power control in multiband cognitive radios," *IEEE Trans. Signal Process.*, vol. 60, no. 10, pp. 5334–5346, Oct. 2012.

[8] A. Mariani, A. Giorgetti, and M. Chiani, "Test of independence for cooperative spectrum sensing with uncalibrated receivers," *IEEE GLOBECOM*, Dec. 2012.

[9] N. Nguyen-Thanh and I. Koo, "Optimal truncated ordered sequential cooperative spectrum sening in cognitive radio," *IEEE Sensors J.*, vol. 13, no. 11, pp. 4188–4195, Nov. 2013.

[10] D. Hamza, S. Assa, and G. Aniba, "Equal gain combining for cooperative spectrum sensing in cognitive radio networks," *IEEE Trans. Wireless Commun.*, vol. 13, no. 8, pp. 4334–4345, Aug. 2014.

[11] T. Q. Duong, T. T. Le, and H. J. Zepernick, "Performance of cognitive radio networks with maximal ratio combining over correlated Rayleigh fading," *IEEE International Conference on Communications and Electronics (ICCE)*, pp. 65–69, Aug. 2010.

[12] Y. Selen, H. Tullberg, and J. Kronander, "Sensor selection for cooperative spectrum sensing," *3rd IEEE Symp. on New Frontiers in DySPAN*, Oct. 2008.

[13] Y. C. Liang, Y. Zeng, E. C. Peh, and A. T. Hoang, "Sensing-throughput tradeoff for cognitive radio networks," *IEEE Trans. Wireless Commun.*, vol. 7, no. 4, pp. 1326–1337, Apr. 2008.

[14] E. Peh and Y. C. Liang, "Optimization for cooperative sensing in cognitive radio networks," *IEEE WCNC*, Mar. 2007.

[15] W. Zhang, R. K. Mallik, and K. B. Letaief, "Optimization of cooperative spectrum sensing with energy detection in cognitive radio networks," *IEEE Trans. Wireless Commun.*, vol. 8, no. 12, pp. 5761–5766, Dec. 2009.

[16] M. Haenggi, "On distances in uniformly random networks," *IEEE Trans. Inf. Theory*, vol. 51, no. 10, pp. 3584–3586, Oct. 2005.

[17] M. Haenggi, J. Andrews, F. Baccelli, O. Dousse, and M. Franceschetti, "Stochastic geometry and random graphs for the analysis and design of wireless networks," *IEEE J. Sel. Areas Commun.*, vol. 27, no. 7, pp. 1029–1046, Sep. 2009.

[18] X. Song, C. Yin, D. Liu, and R. Zhang, "Spatial throughput characterization in cognitive radio networks with threshold-based opportunistic spectrum access," *IEEE J. Sel. Areas Commun.*, vol. 32, no. 11, pp. 2190–2204, Nov. 2014.

[19] S. A. R. Zaidi, M. Ghogho, D. C. Mclernon, and A. Swami, "Achievable spatial throughput in multi-antenna cognitive underlay networks with multi-hop relaying," *IEEE J. Sel. Areas Commun.*, vol. 31, no. 8, pp. 1543–1558, Aug. 2013.

[20] J. Lee, J. G. Andrews, and D. Hong, "Spectrum-sharing transmission capacity," *IEEE Trans. Wireless Commun.*, vol. 10, no. 9, pp. 3053–3063, Sep. 2011.

[21] M. G. Khoshkholgh, K. Navaie, and H. Yanikomeroglu, "Outage performance of the primary service in spectrum sharing networks," *IEEE Trans. Mobile Comput.*, vol. 12, no. 10, pp. 1955–1971, Oct. 2013.

[22] M. Peng, S. Yan, and H. V. Poor, "Ergodic capacity analysis of remote radio head associations in cloud radio access networks," *IEEE Wireless Commun. Lett.*, vol. 3, no. 4, pp. 365–368, Aug. 2014.

[23] C. Lee and M. Haenggi, "Interference and outage in Poisson cognitive networks," *IEEE Trans. Wireless Commun.*, vol. 11, no. 4, pp. 1392–1401, Apr. 2012.

[24] L. T. Tan and L. B. Le, "Joint cooperative spectrum sensing and MAC protocol design for multi-channel cognitive radio networks," *EURASIP J. Wirel. Commun. Netw.*, vol. 2014, no. 1, Dec. 2014.

[25] R. Zhang and Y. C. Liang, "Exploiting multi-antennas for opportunistic spectrum sharing in cognitive radio networks," *IEEE J. Sel. Topics Signal Process.*, vol. 2, no. 1, pp. 88–102, Feb. 2008.

[26] Z. Quan, S. Cui, A. Sayed, and H. V. Poor, "Optimal multiband joint detection for spectrum sensing in cognitive radio network," *IEEE Trans. Signal Process.*, vol. 57, no. 3, pp. 1128–1140, Mar. 2009.

[27] F. Li and Z. Xu, "Sparse bayesian hierarchical prior modeling based cooperative spectrum sensing in wideband cognitive radio networks," *IEEE Signal Process. Lett.*, vol. 21, no. 5, pp. 586–590, May 2014.

[28] R. Zhang, T. J. Lim, Y. C. Liang, and Y. Zeng, "Multi-antenna based spectrum sensing for cognitive radios: A GLRT approach," *IEEE Trans. Commun.*, vol. 58, no. 1, pp. 84–88, Jan. 2010.

[29] L. Wei and O. Tirkkonen, "Analysis of scaled largest eigenvalue based detection for spectrum sensing," *IEEE ICC*, pp. 1–5, Jun. 2011.

[30] A. Kortun, M. Sellathurai, T. Ratnarajah, and C. Zhong, "Distributionn of the ratio of the largest eigenvalue to the trace of complex Wishart matrices," *IEEE Trans. Signal Process.*, vol. 60, no. 10, pp. 5527–5532, Oct. 2012.

[31] Y. He, T. Ratnarajah, J. Xue, E. H. G. Yousif, and M. Sellathurai, "Optimal decision threshold for eigenvalue-based spectrum sensing techniques," *IEEE ICASSP*, May 2014.

[32] I. S. Gradshteyn and I. M. Ryzhik, *Table of integrals, series, and products*, 7th ed., A. Jeffrey and D. Zwillinger, Eds. New York, USA: Academic Press, 2007.

[33] C. R. Stevenson, C. Cordeiro, E. Sofer, and G. Chouinard, "IEEE P802.22 wireless RANs functional requirements for the 802.22 WRAN standard doc.:IEEE 802.22-05/0007r46," *WK3C Wireless LLC*, pp. 1–49, Sep. 2005.

[34] S. Chaudhari, J. Lunden, V. Koivunen, and H. V. Poor, "Cooperative sensing with imperfect reporting channels: Hard decisions or soft decisions?" *IEEE Trans. Signal Process.*, vol. 60, no. 1, pp. 18–28, Jan. 2012.

[35] A. Sahai and D. Cabric, "A tutorial on spectrum sensing: Fundamental limits and practical challenges," *IEEE Symp. New Frontiers DySPAN*, Nov. 2005.

[36] K. Johansson, "Shape fluctuations and random matrices," *Commun. Math. Phys.*, vol. 209, no. 2, pp. 437–476, Feb. 2000.

[37] F. Haddadi, M. M. Mohammadi, M. M. Nayebi, and M. R. Aref, "Statistical performance analysis of MDL source enumeration in array processing," *IEEE Trans. Signal Process.*, vol. 58, no. 1, pp. 452–457, Jan. 2010.

[38] K. M. Wong, Q. Zhang, J. P. Reilly, and P. C. Yip, "On information theoretic criteria for determining the number of signals in high resolution array," *IEEE Trans. Acoust., Speech, Signal Process.*, vol. 38, no. 11, pp. 1959–1971, Nov. 1990.

Yibo He received the B.Eng. degree in Electronic Information Engineering from Zhengzhou University, Zhengzhou, China, in 2011, the M.S. degree in Signal Processing and Communications from the University of Edinburgh, Edinburgh, U.K., in 2012. Since 2013, he has been working toward a Ph.D. degree at Institute for Digital Communications, the University of Edinburgh, U.K. His main research interests focus on cognitive radio networks, stochastic geometry and full-duplex communications.

Jiang Xue received the B.S. degree in Information and Computing Science from the Xi'an Jiaotong University, Xi'an, China, in 2005, the M.S. degrees in Applied Mathematics from Lanzhou University, China and Uppsala University, Sweden, in 2008 and 2009, respectively. Dr. J. Xue received the Ph.D. degree in Electrical and Electronic Engineering from ECIT, the Queen's University of Belfast, U.K., in 2012. He is currently a Research Fellow with the University of Edinburgh, U.K. His main interest lies in the performance analysis of general multiple antenna systems, Stochastic geometry, cooperative communications, and cognitive radio.

Tharmalingam Ratnarajah (A'96-M'05-SM'05) is currently with the Institute for Digital Communications, University of Edinburgh, Edinburgh, UK, as a Professor in Digital Communications and Signal Processing. His research interests include signal processing and information theoretic aspects of 5G wireless networks, full-duplex radio, mmWave communications, random matrices theory, interference alignment, statistical and array signal processing and quantum information theory. He has published over 280 publications in these areas and holds four U.S. patents. He is currently the coordinator of the FP7 projects ADEL (3.7M€) in the area of licensed shared access for 5G wireless networks. Previously, he was the coordinator of the FP7 project HARP (3.2M€) in the area of highly distributed MIMO and FP7 Future and Emerging Technologies projects HIATUS (2.7M€) in the area of interference alignment and CROWN (2.3M€) in the area of cognitive radio networks. Dr Ratnarajah is a Fellow of Higher Education Academy (FHEA), U.K., and an associate editor of the IEEE Transactions on Signal Processing.

Mathini Sellathurai is presently a Reader with the Heriot-Watt University, Edinburgh, U.K. and leading research in signal processing for intelligent systems and wireless communications. Her research includes adaptive, cognitive and statistical signal processing techniques in a range of applications including Radar and RF networks, Network Coding, Cognitive Radio, MIMO signal processing, satellite communications and ESPAR antenna communications. She has been active in the area of signal processing research for the past 15 years and has a strong international track record in multiple-input, multiple-output (MIMO) signal processing with applications in radar and wireless communications research. Dr. Sellathurai has 5 years of industrial research experience. She held positions with Bell-Laboratories, New Jersey, USA, as a visiting researcher (2000); and with the Canadian (Government) Communications Research Centre, Ottawa Canada as a Senior Research Scientist (2001-2004). Since 2004 August, she has been with academia. She also holds an honorary Adjunct/Associate Professorship at McMaster University, Ontario, Canada, and an Associate Editorship for the IEEE Transactions on Signal Processing between 2009-2013 and presently serving as an IEEE SPCOM Technical Committee member. She has published over 150 peer reviewed papers in leading international journals and IEEE conferences; given invited talks and written several book chapters as well as a research monograph titled "Space-Time Layered Processing" as a lead author. The significance of her accomplishments is recognized through international awards, including an IEEE Communication Society Fred W. Ellersick Best Paper Award in 2005, Industry Canada Public Service Awards for contributions in science and technology in 2005 and awards for contributions to technology Transfer to industries in 2004. Dr. Sellathurai was the recipient of the Natural Sciences and Engineering Research Council of Canadas doctoral award for her Ph.D. dissertation.

Faheem A. Khan (M'02) received the Ph.D. degree in electrical and electronic engineering from Queens University Belfast, U.K. in 2012. He is currently a research associate in wireless communications and signal processing at Institute for Digital Communications, The University of Edinburgh, U.K., under the EU funded FP7 project ADEL. He also participated in the past EU FP7 projects, CROWN, HIATUS and HARP. His research interests include cognitive radio networks, 5G wireless networks, millimeter wave communications and cooperative communications.